Good Vibrations: Calculating Excited State Frequencies Using Ground State Self-Consistent Field Models

Ali Abou Taka, Hector H. Corzo, Aurora Pribram–Jones,* and Hrant P. Hratchian*

Department of Chemistry and Biochemistry and Center for Chemical Computation and Theory, University of California, Merced, California 95343, USA

E-mail: apj@ucmerced.edu; hhratchian@ucmerced.edu

Abstract

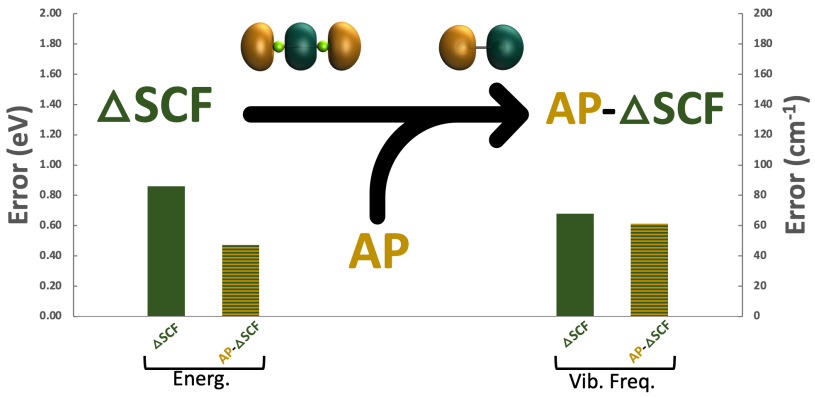

Δ-self–consistent–field (Δ-SCF) methods have proven to be reliable computational tools for the assignment and interpretation of photoelectron spectra of isolated molecules. These results have increased the interest for Δ-SCF techniques for electronic excited states based on improved algorithms that prevent convergence to ground states. In this work, one of these Δ-SCF improved algorithms is studied to demonstrate its ability to explore the molecular properties for excited states. Results from Δ-SCF calculations for a set of representative

molecules are compared with results obtained using time–dependent density functional theory and single substitution configuration interaction method. For the Δ-SCF calculations, the efficacy of a spin–purification technique is explored to remedy some of the spin–contamination presented in some of the SCF solutions. The obtained results suggest that the proposed projection–based SCF scheme, in many cases, alleviates the spin–contamination present in the SCF single determinants, and provides a computational alternative for the efficient exploration of the vibrational properties of excited states molecules.

1 Introduction

Electronic excited states play a critical role in fields as varied as photochemistry, analytical chemistry, materials science, and biology.[1–11] Insights into photochemical and photophysical processes are often reliant on information of excited–state potential energy surfaces. In such cases, electronic excitation lead to geometry changes.[12,13] Based on vibrational modes' dependence on the potential energy surface (PES), variations may generate different vibrations, induce forbidden transitions, or facilitate non–adiabatic coupling.[14,15] Despite advancements in experimental techniques involving exited–state molecules, there is a need for accurate and efficient computational routes to excited–state geometries and electronic structure of molecules.

More precise descriptions of excited states can be obtained by multiconfigurational methods.[16–18] In multiconfigurational methods, the wavefunction is formed based on the ground–state Slater determinant and substituted determinants that are constructed via swaps of occupied with virtual orbitals.In such methods, Slater determinants are weighted by expansion coefficients obtained variationally by diagonalizing the Hamiltonian matrix.[19] These expansion coefficients and the spin–orbitals are further optimized in the SCF, which makes addressing large systems prohibitively expensive computationally .

On the other hand, the Kohn–Sham framework offers a density–based approach framed as time dependent Density Functional Theory (TD-DFT).[20–23] In TD-DFT, the complicated many–body time-dependent Schrödinger equation is reformulated by a set of time–dependent single–

particle equations whose orbitals yield the same time–dependent density.Due to its efficiency and relatively black box implementation, TD-DFT has been the method of choice for most excited state calculations and has achieved massive success in different areas.[24–39]

Among the methods based on Slater determinants, Configuration Interaction (CI) with only single orbital substitutions and TD-DFT are among the candidates for addressing large molecular systems. In many cases, these models provide enough information for the characterization of excited–state systems, yet they both suffer from limitations. Configuration Interaction Singles (CIS) neglects important contributions to electron correlation and, since only single substitutions are considered, CIS cannot describe doubly excited states.[40] On the other hand, the available TD-DFT approximations give substantial errors for excited states of molecules with extended π–systems,[41,42] and cannot accurately describe double excitations or charge–transfer (CT) states.[43–45]

One way to describe excited–states is through Δ-SCF methods.In Δ-SCF methods, the excitation energy is obtained by taking the difference between two SCF solutions corresponding to the excited and ground state.

Variational computational chemistry methods based on Slater determinants built of spin–orbitals provide a foundation for defining and computing SCF, configuration–interaction, and other types of post Hartree–Fock wave–function approximations . In general, computational quantum chemistry methods based on spin–orbitals produce reasonable approximations for the description of molecular excited–states.[46–48] In particular, computational methods based on the Hartree–Fock (HF) and Kohn-Sham (KS) models have proven effective in calculating binding energies, excitation energies, and corresponding transition probabilities.

In recent years, Gill and coworkers reintroduce the idea of SCF calculations for excited–states using the maximum overlap method (MOM), which was further upgraded to the initial maximum overlap method (IMOM).[49,50] This concept has been used to explore various electronic and structural properties in molecules.[49–59] In such methodologies, standard ground–state SCF algorithms are used to find a stationary point in the SCF space that maximizes the overlap with an initial guess set of occupied molecular orbitals. However, these low–cost approaches often

suffer from a number of challenges, including convergence difficulties and variational collapse. Recently, the projected initial molecular overlap method (PIMOM), an interpretive tool based on MOM and IMOM, was shown to overcome some of the challenges of the previous algorithms and providing better chemical and physical understanding for the maximum overlap models.cite PIMOM In fact, the projection based framework provides a convenient connection to population analysis.cite PIMOM

Although Δ-SCF methods provide a computationally feasible approach, they may result in broken–symmetry (BS) solutions. The BS determinant often shows a mixture of different spin–pure configurations and results in spin contaminated states. Errors corresponding with these solutions may results in a significant change in the energies, demanding a way to remedy those errors. Correcting spin contaminated states can be done using spin–projection methods. Among other methods, the proposed approximate projection (AP) technique by Yamaguchi has been successfully used in correcting spin–contamination errors.[60–65]

In this work, the usage of the PIMOM framework for geometry optimization and frequency calculation of excited–states molecules is explored. An overview of the method and computational details are given in Section 2. Assessment of the method in evaluating properties of optimized electronic excited states as well as exploring the effect of approximate spin–purification procedure is explored in Section 3. Final remarks and conclusions are given in Section 4.

2 Methods

2.1 Initial Projected Maximum Overlap Method

Standard self–consistent–field eigenstates solutions are achieved by iteratively solving the following equation,

$$\mathbf{FC} = \mathbf{SC}\varepsilon \tag{1}$$

where **F** is the Fock matrix, **C** is the molecular orbital (MO) coefficients matrix, **S** is the overlap matrix in the atomic orbital basis, and ε is the orbital energy vector. The conventional way of solving this eigenvalue problem is by diagonalizing **F**, obtaining a new set of MOs and filling the lowest MOs using the Aufbau principle until convergence. SCF excited–state solutions may be produced by imposing additional control over the spin–orbitals through symmetry restrictions, overlap matching, inclusion of additional constraints on Lagrangian functions and other means.[66–74] A practical strategy for accessing excited–states solutions may be incorporated in the Δ-SCF methods where a projector operator that dictates the orbitals' ordering is used instead of the Aufbau principle. The Δ-SCF method's algorithm begins by defining the target system's density projector, $\mathscr{P}^{\text{target}}$,

$$\mathscr{P}^{\text{target}} = \sum_{i}^{N} \left|\varphi_i^{\text{target}}\right\rangle \left\langle\varphi_i^{\text{target}}\right|. \tag{2}$$

In the MO basis of the current SCF cycle, Eq. (2) reads

$$P_{pq}^{\text{target}} = \langle p \,|\mathscr{P}|\, q\rangle = \sum_{i} \left\langle p \;\middle|\; i^{\text{target}}\right\rangle \left\langle i^{\text{target}} \;\middle|\; q\right\rangle, \tag{3}$$

Eq. (3) may be rewritten as

$$P_{pq}^{\text{target}} = \sum_{i}\sum_{\mu\nu}\sum_{\lambda\sigma} C_{\mu p} \langle \mu \mid \lambda\rangle C_{\lambda i}^{\text{target}} C_{\sigma i}^{\text{target}} \langle \sigma \mid \nu\rangle C_{\nu q}, \tag{4}$$

where $S_{\mu\nu} = \langle \mu \mid \nu\rangle$ are the AO overlap matrix elements. In Eq. (4), the target density matrix in the AO basis may be expressed as $P_{\mu\nu}^{\text{target}} = \sum_i C_{\mu i}^{\text{target}} C_{\nu i}^{\text{target}}$. Thus, Eq. (4) may be written in matrix form as

$$\mathbf{P}_{(MO)}^{\text{target}} = \mathbf{C}^T \mathbf{S} \mathbf{P}^{\text{target}} \mathbf{S} \mathbf{C}, \tag{5}$$

where the subscript "MO" has been included to clearly indicate that the resultant density matrix is given in the current MO basis. Using this equation, the metric employed in the Δ-SCF method to order the MO orbitals is given by

$$s_p = \sum_{q} P_{pq}^{\text{target}}. \tag{6}$$

Similar to the IMOM procedure, different SCF excited–state solutions are accessed by generating s_p values using an initial vector state guess.[50] Δ-SCF methods add an additional constraint to the SCF procedure by anchoring the initial guess vector state and projecting it in the vector state of each SCF cycle. Since the projection is defined using an initial vector space, it is crucial that the initial guess resembles the desired excited state.

2.2 Approximate Projection Method

The effect of spin contamination on the calculated electronic excited states is investigated. For this purpose, the Yamaguchi approximate projection (AP) model was employed.[60] Our group has expanded the AP model to include analytical first and second derivatives.[75,76] In fact, several works have shown the effectiveness of this model and demonstrated the condition for which this model is suitable.[64,65,77,78] To carry out AP calculations, two converged determinants are required: (1) a broken–symmetry state, i.e.,the contaminated state, and (2) a spin–pure high–spin state. Using those determinants, the AP energy expression is constructed as follows:

$$E_{AP} = \alpha E_{LS} + (1-\alpha) E_{HS} \tag{7}$$

where

$$\alpha = \frac{\langle S^2_{HS} \rangle - S_{z,LS}(S_{z,LS}+1)}{\langle S^2_{HS} \rangle - \langle S^2_{LS} \rangle} \tag{8}$$

Subscript low–spin (LS) refers to (broken–symmetry) low-spin state, and high–spin (HS) corresponds to (spin-pure) high-spin state.

$$\alpha^* = \frac{\langle S^2_{\text{pure}} \rangle - \langle S^2_{\Delta\text{-SCF}} \rangle}{1 - \langle S^2_{\Delta\text{-SCF}} \rangle} \times 100 \tag{9}$$

Using the contamination percentage α^* shown in Eq. 9, excited states suffering from heavy spin contamination were identified and assessed for spin purification.

2.3 Computational Details

The results obtained with Δ-SCF methods are reported below and compared with results obtained with CIS, TD-DFT, and experimental data. All Δ-SCF ground and excited–state structures were optimized using Becke's three–parameter hybrid functional with Lee–Yang–Parr correlation (B3LYP)[79] and Hartree–Fock method.[80] Four different basis sets have been used, 6-311G, 6-311++G(d,p),[81–85] aug-cc-pVDZ, and aug-cc-pVTZ.[86–93] All Δ-SCF results were obtained using the PIMOM method as implemented in a local development version of Gaussian.[94]

Molecular geometries for ground–state structures were optimized using standard methods[95] and the reported potential energy minima were verified using analytical second–derivative calculations. The ground–state minimum structures were used as a starting point for excited state optimization using Δ-SCF, CIS, and TD-DFT methods. Those were also verified using analytical second–derivative calculations. Initial electronic structure guesses for Δ-SCF calculations were generated by permuting orbitals of the ground–state converged wavefunction resembling the desired excited–state. AP–Δ-SCF calculations and optimizations were carried out on the spin contaminated systems and verified using analytical second–derivative calculations.

3 Results and Discussion

3.1 Data Set

Excited–state computation tools are expensive and somewhat limited compared to the ground–state toolbox, especially for polyatomic molecules. The purpose of this study is to investigate the modified SCF algorithm, PIMOM, to access different excited states, as well as describe their spectroscopic properties in specific, fundamental vibrational frequencies. This data set was chosen based on available experimental results from gas–phase spectroscopy and can be carried out using the two well–known, relatively feasible, CIS and TD-DFT methods.[96–105] Furthermore, this data set was chosen to contain a variety of types of excited states and spin multiplicities. The test set

used here contains di- and polyatomic molecules.

3.2 Adiabatic Excitation Energies

Table 1: Calculated adiabatic excitation energies (eV) using TD-DFT and Δ-DFT in comparison with the experiment.

		6–311G		6–311++G(d,p)	
Sys	**Exp.**	**TD-DFT**	**Δ-DFT**	**TD-DFT**	**Δ-DFT**
BH	2.87	2.75	1.67	2.74	1.69
BF	6.34	6.13	4.24	6.09	4.31
SiO	5.31	4.83	4.12	5.20	4.44
CO	8.07	7.51	6.21	7.95	6.60
N_2	8.59	7.92	6.97	8.50	7.53
ScO	2.04	1.35	1.77	2.00	1.72
BeH	2.48	2.58	2.37	2.56	2.35
AsF	3.19	2.95	2.96	2.87	2.87
NH	3.70	3.98	3.64	3.90	3.61
CrF	1.01	1.47	1.44	1.25	1.23
CuH	2.91	3.35	2.46	2.98	2.70
Li_2	1.74	1.93	1.09	1.93	1.07
Mg_2	3.23	3.45	2.32	3.26	2.26
PH_2	2.27	2.19	2.13	2.34	2.24
CH_2S	2.03	2.04	1.64	2.06	1.67
C_2H_2	5.23	4.92	4.64	4.70	4.38
$C_2H_2O_2$	2.72	2.21	1.93	2.42	2.12
HCP	4.31	3.91	3.74	3.86	3.60
HCN	6.48	6.02	5.70	5.95	5.59
C_3H_4O	3.21	2.98	2.64	3.15	2.78
CH_2O	3.49	3.36	2.79	3.59	3.01
CCl_2	2.14	-[1]	1.36	1.99	1.29
SiF_2	5.34	4.85	3.79	5.31	3.96
MAE		**0.33**	**0.76**	**0.17**	**0.68**
RMSE		**0.38**	**0.96**	**0.23**	**0.86**

Δ-SCF methods,[106,107] especially maximum overlap methods, have shown great success in calculating vertical excitation energies.[49,50,108–111] Table 1 shows the adiabatic excited state energies calculated using TD-DFT and Δ-B3LYP with the four basis sets considered. Δ-B3LYP yielded comparable results to TD-DFT, where TD performed better than Δ-B3LYP with mean average errors between 0.42 and 0.52 eV relative to experiment.

Upon increasing the basis set from 6–311G to 6–311++G(d,p), the mean absolute error (MAE)

Table 2: Calculated adiabatic excitation energies (eV) using CIS and Δ-HF in comparison with the experiment.

		6–311G		6–311++G(d,p)	
Sys	**Exp.**	**CIS**	**Δ-HF**	**CIS**	**Δ-HF**
BH	2.87	3.03	1.64	2.89	1.50
BF	6.34	6.49	4.39	6.54	4.51
SiO	5.31	5.23	2.90	6.09	3.74
CO	8.07	8.01	6.36	8.74	7.00
N_2	8.59	8.65	7.25	9.45	8.06
ScO	2.04	2.30	1.60	2.07	2.05
BeH	2.48	2.78	2.64	2.76	2.64
AsF	3.19	3.83	3.57	3.76	3.44
NH	3.70	4.05	3.79	4.18	3.84
CrF	1.01	1.15	0.98	0.99	0.60
CuH	2.91	3.97	1.70	3.93	1.42
Li_2	1.74	2.11	0.96	2.10	0.92
Mg_2	3.23	3.59	2.69	3.34	2.46
PH_2	2.27	2.33	2.20	2.68	2.38
CH_2S	2.03	1.99	0.58	2.71	0.90
C_2H_2	5.23	4.68	4.07	4.49	3.71
$C_2H_2O_2$	2.72	3.24	3.12	3.56	3.30
HCP	4.31	3.46	3.03	3.59	2.95
HCN	6.48	5.54	4.88	5.95	4.78
C_3H_4O	3.21	4.36	1.29	4.58	1.67
CH_2O	3.49	3.99	1.51	4.10	1.66
CCl_2	2.14	2.08	0.69	2.40	1.07
SiF_2	5.34	5.69	3.97	5.96	4.09
MAE		**0.41**	**1.07**	**0.55**	**0.97**
RMSE		**0.52**	**1.27**	**0.63**	**1.13**

of calculated adiabatic excitation energies (AEEs) of TD-DFT and Δ-B3LYP decreased by 0.15 eV and 0.08 eV, respectively. This improvement can be explained by the addition of polarization and diffuse functions, which provides a better qualitative description for electronic excited states.[112] A similar behavior is observed using Dunning's basis sets, for which the MAE for both TD and Δ-SCF–based calculation decreased by 0.05 upon increasing the basis set from 6-311G to 6-311++G(d,p) and by 0.04 eV upon increasing the basis set from aug-cc-pVDZ, and aug-cc-pVTZ. This improvement is smaller than the one observed with the Pople basis sets, which is not unexpected since both Dunning basis sets use a larger number of polarization and diffuse functions.

In the case of CIS, the MAE ranges between 0.41 and 0.55 eV, which is smaller than the MAE

obtained using Δ-HF, 1.00–1.14 eV, as reported in Table 2. Upon adding diffuse and polarization functions, unlike TD-DFT, the excitation energy accuracy decreased, where the MAE obtained using 6–311G is smaller than the MAE of 6–311++G(d,p) by 0.14 eV. On the other hand, for correlation consistent basis sets, a smaller difference is observed, 0.05 eV, favoring the larger basis set. On the other hand, Δ-HF showed an improved accuracy as the basis set size is increased, where MAE decreased by 0.14 eV with the Pople basis set and 0.12 eV with the correlation consistent basis sets.

Absolute errors in TD-DFT and Δ-B3LYP adiabatic excitation energies are noticeably smaller than those found with CIS and Δ-HF, which is expected due to the correlation effects included in DFT. The AEE obtained using Δ-SCF of the investigated systems here showed an underestimation, which can be attributed to several factors, such as incomplete treatment of relaxation and correlation effect, and spin contamination. In general, the correct description of excited states requires a balanced treatment of orbital relaxation and correlation effects.

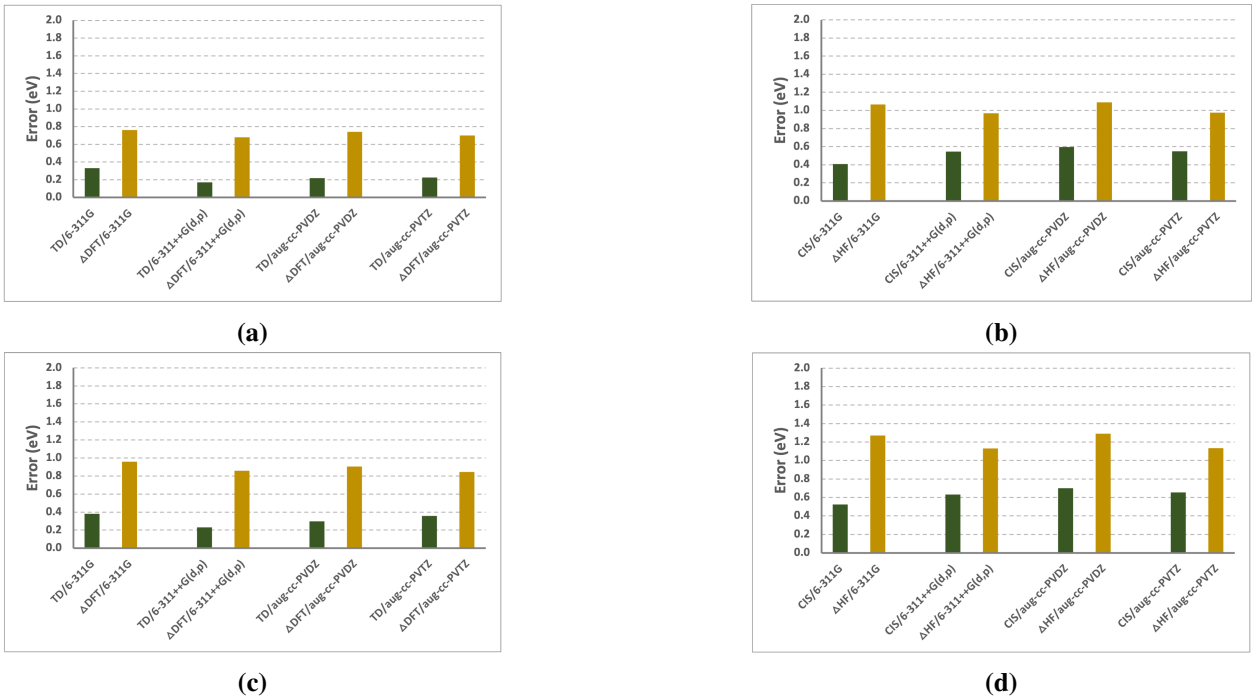

Figure 1: Errors in adiabatic excitation energies obtained using (a) Δ-DFT and TD-DFT and (b) Δ-HF and CIS with respect to experiment. RMSE of the adiabatic excitation energies obtained using (c) Δ-DFT and TD-DFT and (d) Δ-HF and CIS with respect to experiment are also reported.

3.3 Vibrational Analysis of the Excited States

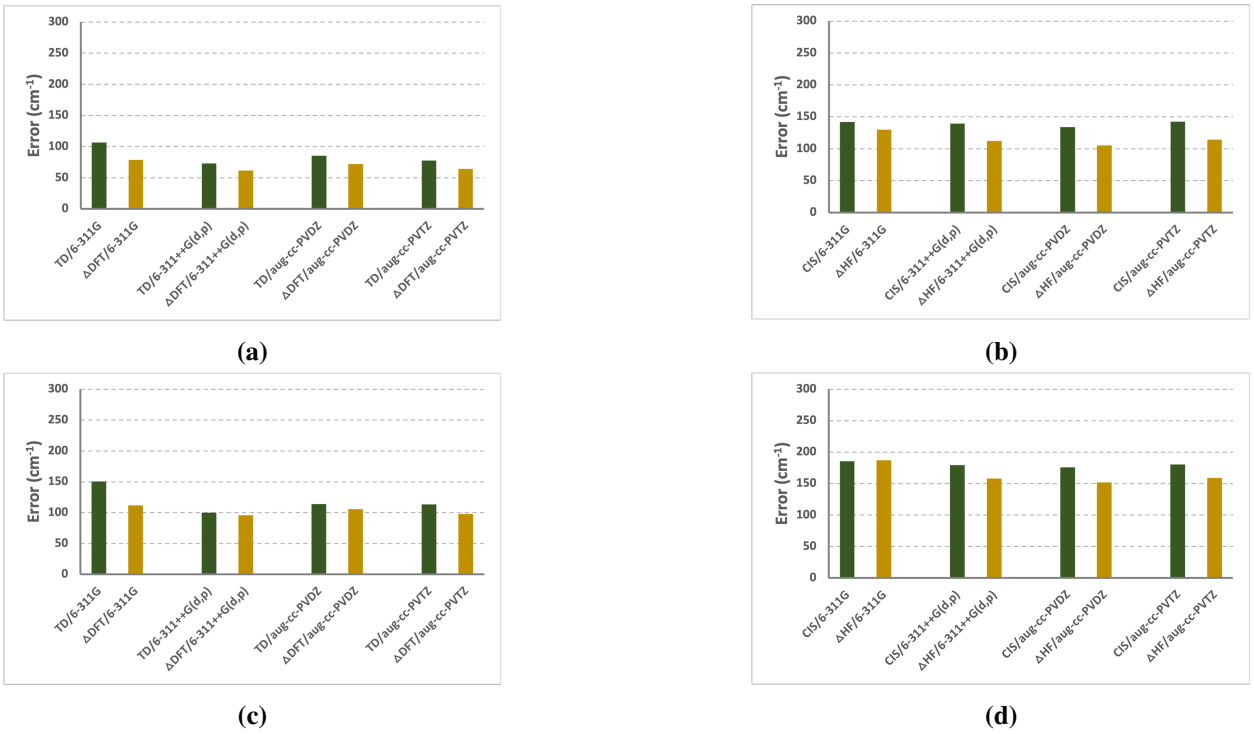

Figure 2: Mean absolute errors in vibrational frequencies obtained using (a) Δ-DFT and TD-DFT and (b) Δ-HF and CIS with respect to experiment. RMSE is also reported for (c) Δ-DFT and TD-DFT and (d) Δ-HF and CIS.

The computed excited–state frequencies from all methods gave smaller relative errors than the relative errors of the adiabatic excitation energies. Unlike the computed excitation energies, the mean absolute errors obtained using Δ-B3LYP are less than those obtained using the TD-DFT methodology by 11–28 cm^{-1}.

The effect of basis set is less significant in the accuracy of the calculated vibrational frequencies. In the case of the Pople basis sets, the addition of diffuse and polarization functions lowered the MAE by 34 cm^{-1} and 17 cm^{-1} for TD and Δ-B3LYP , respectively. Dunning style basis sets showed a similar behavior with an increase in accuracy of 8 cm^{-1} for both TD and Δ-B3LYP , respectively. Pople's basis set, 6–311++G(d,p), gave the lowest MAE of 62 cm^{-1} with Δ-B3LYP and 73 cm^{-1} with TD.

In general, Δ-B3LYP gave superior results to TD with all the basis sets considered. The

lowest MAE was reported using 6–311++G(d,p); thus the discussion will be focused on this basis set. In cases such as the 1 $^1\Sigma_u^+$ state of Mg_2, the $\nu_2(a_1)$ mode of the 1^1B_1 of CCl_2, and the $\nu_4(a_1)$ mode of the 1 $^1A''$ state of CH_2O, Δ-B3LYP yielded remarkably more accurate vibrational frequencies than TD by 22, 36, and 14%, respectively. These results may be due to the incomplete TD-DFT treatment of the correlation effects in the excited states arising from non–valence and degenerate.orbitals[113] On the other hand, in the case of the 1 $^1\Sigma_u^+$ of Li_2 and the 1 $^1\Pi$ of CO, Δ-B3LYP gave higher error in the computed vibrational frequencies by 16% and 10%, respectively. These results may be connected to the indirect treatment of orbital relaxation and correlation effects in the Δ-B3LYP calculation where, due to the nature of the calculation, a direct, balanced treatment of these effect can not be achieved.

Unsurprisingly, CIS and Δ-HF performed worse than TD-DFT and Δ-DFT for calculating excited sate vibrational frequencies. The MAE of CIS ranges between 139 cm^{-1} and 142 cm^{-1}, higher than the MAE of TD, which ranges between 73 cm^{-1} and 107 cm^{-1}. These results may be attributed to the exchange–correlation effects in DFT. This gives DFT a clear advantage over the CIS and HF methods. Δ-HF displayed a MAE that ranges between 112 cm^{-1} and 139 cm^{-1}, significantly higher than the MAE obtained using DFT, which attained an uppermost MAE of 79 cm^{-1}.

Δ-HF performed similarly or better than CIS in all the cases considered in this data set. For example, for the $\nu_3(a')$ mode of the CH_2S 1 $^1A_2$ excited state, CIS resulted in a 30% error, much higher than the error resulting from Δ-HF, 9%. Also, CIS sustained large errors in describing the excited states of the carbonyl compounds, such as C_3H_8O, CH_2O, and $(CHO)_2$, unlike HF, where the errors were much less for most of the vibrational modes. These examples demonstrate well the advantages and disadvantages of describing excited states using CIS, TD or Δ-SCF. In most cases, Δ-SCF methods presented similar or somewhat improved accuracy in calculating the vibrational frequencies of the considered excited states than CIS and TD-DFT. Detailed tables showing the behavior observed by the different models considered can be found in the supporting information (tables S1-S16).

3.4 Spin Contamination

In many cases, excited states obtained using the Δ-SCF approach are spin contaminated, motivating the examination of spin purification methods.[59,60,114–116] Among the different spin-purification schemes, the multiplet splitting formula was recently reintroduced to purify open-shell singlet excited state energies.[59] For our purposes, we considered a variation of this scheme, the approximate projection model of Yamaguchi and co–workers,[60] as implemented and extended by our lab.[64,65,75–78] Using Eq. 9 and a threshold of 5% spin contamination, 17 systems were identified as being spin contaminated with Δ-DFT and explored using the AP model. It is important to note that the AP model is expected to behave well only for situations where the spin contaminated state has only one higher spin contaminant to be projected out. With this in mind, we identified C_2H_2 and CO as systems inappropriate for this AP approach. Using HF with all the basis sets considered, the triplet state of C_2H_2 exhibited geometric symmetry breaking, C_{2_h} to C_s, and the different symmetries of the low- and high-spin states caused difficulties in AP convergence. Using HF/6–311G, CO was also excluded since the triplet also showed significant spin contamination. AP showed a similar performance with all basis sets considered. Thus, we will limit our discussion to the 6-311++G(d,p) basis set. Full details obtained using the other model chemistries are provided in the supporting information (tables S1-S16).

As reported recently, the effect of the AP model on energies was significant for all model chemistries considered.[59] As shown in Figs. 3 and 4, the MAE for Δ-SCF methods decreased by $\sim$0.4 eV for Δ-DFT and $\sim$0.5 eV for Δ-HF model chemistries. For the specific cases of BF and SiF_2 , AP–Δ-DFT reduced the error by 0.95 and 0.76 eV, respectively, using 6–311++G(d,p) basis. This highlights the efficacy of AP in treating multi–determinantal states. A similar behavior has been observed for the AP–Δ-HF method, where the error of BF and SiF_2 dropped by 1.63 and 0.67 eV, respectively. On the other hand, it is well known that Δ-SCF excitation energies for open–shell singlets, despite the spin contamination, are often unexpectedly accurate.[49,50,108] This is observed in the cases of CuH, where the error with AP dropped from 0.21 eV to 0.09 eV, and CH_2S, where the error decreased by 0.08 eV to reach 0.28 eV.

The noted improvement in the energetics upon spin purification using AP was not observed to the same extent with frequencies(Figs. 3 and 4). AP showed a slight improvement on the calculated vibrational frequencies when diffuse and polarization functions are included in the basis sets, where the MAE decreased by $\sim$4 cm^{-1} and the RMSE decreased by $\sim$11 cm^{-1}. However, in the case of 6–311G, the MAE and RMSE increased by $\sim$12 cm^{-1}. Interestingly, both Δ-DFT and AP–Δ-DFT perform better than TD-DFT relative to experiment (see Fig. 3). On the other, the MAE of the frequencies obtained by AP–Δ-HF, was $\sim$4 cm^{-1} higher than the Δ-HF method, but the RMSE was $\sim$10 cm^{-1} better than Δ-HF method. This suggest that for extreme cases, where the error is high, AP–Δ-HF preformed better than Δ-HF. In brief, it is safe to say that AP–Δ-SCF is expected to perform comparably to Δ-SCF methods, yet some caution must be taken based on the system under investigation itself. These results are expected and in agreement with a previous study that suggest that this spin projection technique often does not result in large structural changes but can give meaningful changes in energy.[65]

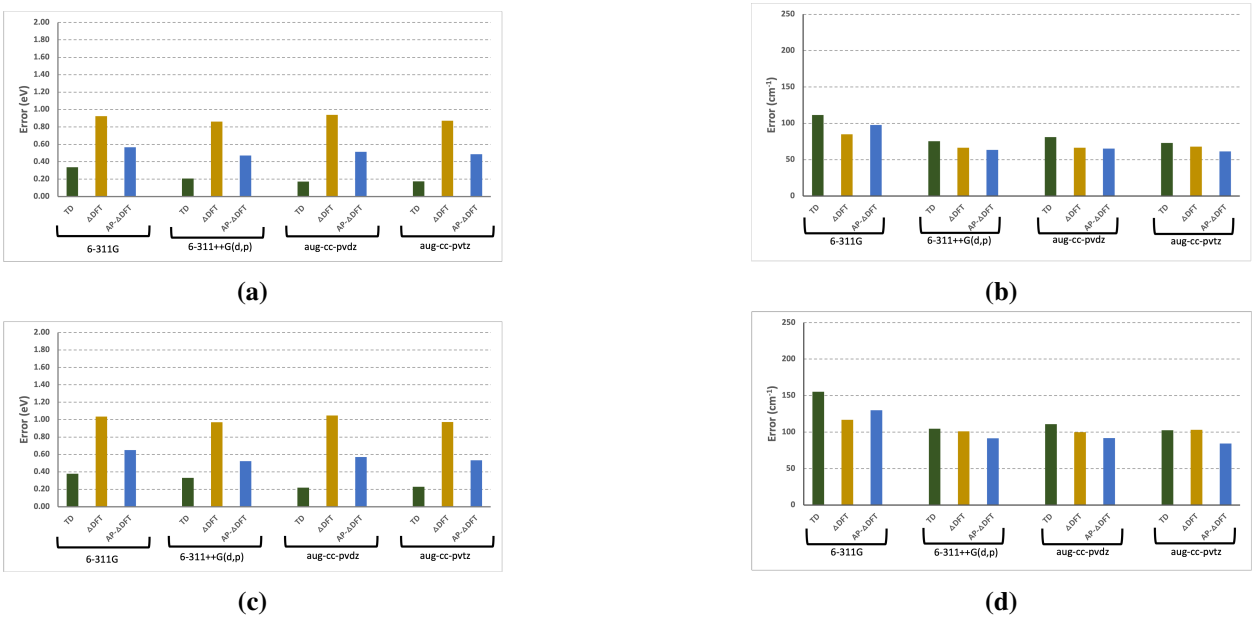

Figure 3: Mean absolute errors in Adiabatic Excited Energies and vibrational frequencies obtained using (a) & (b) Δ-DFT and TD-DFT. RMSE is also reported for the same models (c) & (d).

Table 3: Adiabatic excitation energies before and after approximate projection on systems with Spin contamination above 5%.6-311++G(d,p) basis set was used.

Sys.	Exp.	TD	Δ-B3LYP	AP–Δ-B3LYP	CIS	Δ-HF	AP–Δ-HF
BH	**2.87**	2.74	1.69	2.30	2.89	1.50	2.68
BF	**6.34**	6.09	4.31	5.26	6.54	4.51	6.54
SiO	**5.31**	5.20	4.44	4.83	6.09	3.74	3.97
CO	**8.07**	7.95	6.60	7.37	8.74	7.00	8.63
N_2	**8.59**	8.50	7.53	8.03	9.45	8.06	8.83
CuH	**2.91**	2.98	2.70	3.00	3.93	1.42	1.93
Li_2	**1.74**	1.93	1.07	1.21	2.10	0.92	1.47
CCl_2	**2.14**	1.99	1.29	1.81	2.40	1.07	2.18
CH_2S	**2.03**	2.06	1.67	1.75	2.71	0.90	0.92
Mg_2	**3.23**	3.26	2.26	2.70	3.34	2.46	3.79
C_2H_2O	**2.72**	2.42	2.12	2.31	3.56	3.30	3.31
HCP	**4.31**	3.86	3.65	3.83	3.59	2.95	3.26
CH_2O	**3.49**	3.59	3.01	3.17	4.10	1.66	1.76
C_3H_4O	**3.21**	3.15	2.78	2.87	4.58	1.67	1.73
SiF_2	**5.34**	5.31	3.96	4.72	5.96	4.09	5.92
HCN	**6.48**	5.95	5.59	5.85	5.95	4.78	5.23
C_2H_2	**5.23**	4.70	4.38	4.61	4.49	3.71	-
MAE		**0.17**	**0.86**	**0.47**	**0.63**	**1.22**	**0.76**
RMSE		**0.22**	**0.97**	**0.52**	**0.70**	**1.29**	**0.91**

4 Remarks and Conclusion

4.1 Generating Initial Guess

In MOM–based methods, starting with an initial guess that resembles the desired excited state is crucial to locating it. Previous considerations into the nature of the excited state and its symmetry are the quickest and easiest way to access the desired solution using PIMOM. An orbital permutation from the reference ground state to match the excited state in nature and symmetry suffices in most cases as an initial guess for the PIMOM framework. Nevertheless, in cases where multiple determinants are important for the description of the excited state, any of those are an option for generating the initial guess. For instance, consider the $1^1\Pi$ excited state of SiO. TD-DFT shows three configurations involved in representing this excitation, as follows: an amplitude of 0.17162 for the $11\alpha \rightarrow 13\alpha$ determinant, 0.67339 for the $11\alpha \rightarrow 12\alpha$ determinant, and -0.12437 for the

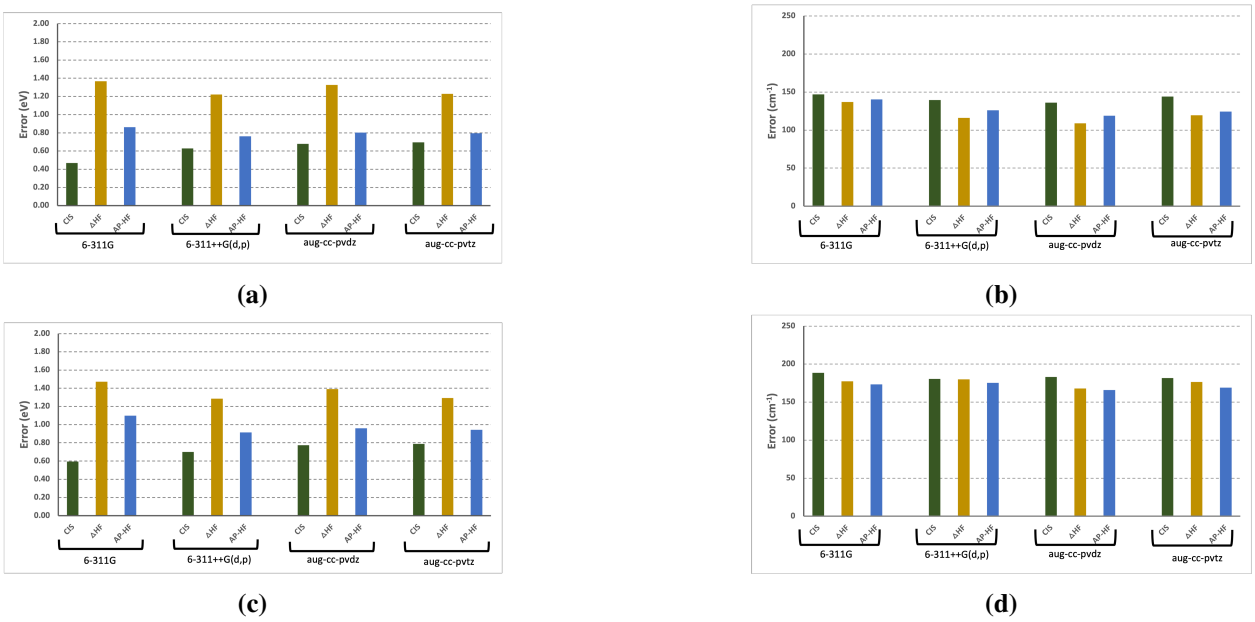

Figure 4: Mean absolute errors in Adiabatic Excited Energies and vibrational frequencies obtained using (a) & (b) Δ-SCF, and CIS. RMSE is also reported for the same models (c) & (d).

$8\alpha \rightarrow 12\alpha$ determinant. Generating an initial guess by permuting either orbital 11α with orbital 12α or orbital 11α with orbital 13α , led to a $1^1\Pi$ excited states with a 4.44 eV excitation energy. However, permuting orbital 8α with orbital 12α let to a $1^1\Pi$ excited state located at 8.20 eV above the ground state. Clearly, either one of the first two permutations led to the correct state. However, in the last solution, though the symmetry of the state may be correct, the energy is off, thus not yielding the desired targeted state. Importantly, we note that using the Natural Transition Orbital (NTO) model to characterize the state, and using those orbitals as initial guess orbitals, led us to the correct state in all cases, including this one. We suggest the NTO model as an approach for generating initial states, particularly in instances where there is no clear one electron transition in the canonical molecular orbital basis.

4.2 Summary

In this paper, we presented a Δ-SCF approach using the PIMOM framework to access adiabatic excited states and describe fundamental properties such as vibrational frequencies. Although TD-DFT and CIS provided a slightly better energetics than PIMOM, the excited vibrational frequencies

obtained with PIMOM were in better agreement with the experiment than either TD-DFT or CIS. The AP model improved the AEE for both DFT and HF and did not have a significant effect on the vibrational frequencies. Since SCF calculations are more affordable than other available excited–state methods, especially for exploring large systems, PIMOM presents a viable computational approach for modeling excited states molecular properties at ground–state computational cost. This work shows the significance of using the AP model to correct the adiabatic excitation energies with having minimal effect on the calculated frequencies. Given the results showed in this work, AP-Δ-SCF technique results in a comparable performance and lower computational cost to single reference excited state models such as, CIS and TD-DFT.

Supporting Information Available

See the supplementary material for details regarding excitation energies and vibrational frequencies summarized in Tables S1–S16. All optimized structures are also provided in the SI.

Acknowledgement

The authors gratefully acknowledge the Department of Energy, Office of Basic Energy Sciences CTC and CPIMS programs (APJ and HPH; Award DE-SC0014437) for supporting this work. Computing time was provided in part by the MERCED cluster at UC Merced, which was also supported by the National Science Foundation (HPH; Award ACI-1429783).

References

(1) Jouvet, C.; Boivineau, M.; Duval, M. C.; Soep, B. Photochemistry in excited states of van der Waals complexes. *J. Phys. Chem.* **1987**, *91*, 5416–22, CAPLUS AN 1987:565195(Journal).

(2) Hashimoto, H.; Yanagi, K.; Yoshizawa, M.; Polli, D.; Cerullo, G.; Lanzani, G.; De Silvestri, S.;

Gardiner, A. T.; Cogdell, R. J. The very early events following photoexcitation of carotenoids. *Arch. Biochem. Biophys.* **2004**, *430*, 61–69.

(3) Stufkens, D. J.; Aarnts, M. P.; Nijhoff, J.; Rossenaar, B. D.; Vlcek, A. J. Excited states of metal-metal bonded diimine complexes vary from extremely long lived to very reactive with formation of radicals or zwitterions. *Coord. Chem. Rev.* **1998**, *171*, 93–105.

(4) Cilento, G.; Adam, W. Photochemistry and photobiology without light. *Photochem. Photobiol.* **1988**, *48*, 361–8.

(5) Mittal, J. P. Excited states and electron transfer reactions of fullerenes. *Pure Appl. Chem.* **1995**, *67*, 103–10.

(6) Tuna, D.; Sobolewski, A. L.; Domcke, W. Electronically excited states and photochemical reaction mechanisms of b-glucose. *Phys. Chem. Chem. Phys.* **2014**, *16*, 38–47.

(7) Endicott, J. F. The photophysics and photochemistry of coordination compounds. Inorg. Electron. Struct. Spectrosc. 1999; pp 291–341.

(8) Obukhov, A. E. Excited states, generation of light and photoprocesses in series of complex N,O, S polyatomic molecules. *Proc. SPIE - Int. Soc. Opt. Eng.* **1995**, *2370*, 268–73.

(9) Klessinger, M.; Michl, J.; Editors., *Excited States and Photochemistry of Organic Molecules.*; VCH, 1995; p 544 pp., Copyright (C) 2020 American Chemical Society (ACS). All Rights Reserved.

(10) Herman, M. S. Studies on excited states and reactive intermediates: enthalpies, kinetics and reaction volume changes. Ph.D. thesis, 1992.

(11) Scharf, H. D.; Fleischhauer, J. Nature, multiplicity, and properties of excited states in photoreactions of organic molecules. Method. Chim. 1974; pp 650–66.

(12) To, W.-P.; Chan, K. T.; Tong, G. S. M.; Ma, C.; Kwok, W.-M.; Guan, X.; Low, K.-H.; Che, C.-M. Strongly Luminescent Gold (III) Complexes with Long-Lived Excited States: High Emission Quantum Yields, Energy Up-Conversion, and Nonlinear Optical Properties. *Angew. Chem. Int. Ed.* **2013**, *52*, 6648–6652.

(13) Eastwood, D.; Gouterman, M. Porphyrins: Xviii. luminescence of (co),(ni), pd, pt complexes. *J. Mol. Spectrosc.* **1970**, *35*, 359–375.

(14) Vlček Jr, A.; Záliš, S. Modeling of charge-transfer transitions and excited states in d6 transition metal complexes by DFT techniques. *Coord. Chem. Rev.* **2007**, *251*, 258–287.

(15) Dierksen, M.; Grimme, S. Density functional calculations of the vibronic structure of electronic absorption spectra. *J. Chem. Phys.* **2004**, *120*, 3544–3554.

(16) McDouall, J. J.; Peasley, K.; Robb, M. A. A simple MC SCF perturbation theory: Orthogonal valence bond Møller-Plesset 2 (OVB MP2). *Chem. Phys. Lett.* **1988**, *148*, 183–189.

(17) Andersson, K.; Malmqvist, P.-Å.; Roos, B. O. Second-order perturbation theory with a complete active space self-consistent field reference function. *J. Chem. Phys.* **1992**, *96*, 1218–1226.

(18) Buenker, R. J.; Peyerimhoff, S. D.; Butscher, W. Applicability of the multi-reference double-excitation CI (MRD-CI) method to the calculation of electronic wavefunctions and comparison with related techniques. *Mol. Phys.* **1978**, *35*, 771–791.

(19) Szabo, A.; Ostlund, N. S. *Modern quantum chemistry: introduction to advanced electronic structure theory*; Courier Corporation, 2012.

(20) Marques, M. A.; Gross, E. K. Time-dependent density functional theory. *Annu. Rev. Phys. Chem.* **2004**, *55*, 427–455.

(21) Furche, F.; Burke, K. Time-Dependent Density Functional Theoryin Quantum Chemistry. *Annu. Rep. Comput. Chem.* **2005**, *1*, 19–30.

(22) Maitra, N. T.; Burke, K.; Appel, H.; Gross, E.; van Leeuwen, R. *Ten topical questions in time-dependent density functional theory*; University of Groningen, The Zernike Institute for Advanced Materials, 2002.

(23) Gross, E.; Dobson, J.; Petersilka, M. Density functional theory of time-dependent phenomena. In *Density functional theory II*; Springer, 1996; pp 81–172.

(24) Coe, B. J.; Harries, J. L.; Helliwell, M.; Jones, L. A.; Asselberghs, I.; Clays, K.; Brunschwig, B. S.; Harris, J. A.; Garín, J.; Orduna, J. Pentacyanoiron (II) as an electron donor group for nonlinear optics: Medium-responsive properties and comparisons with related pentaammineruthenium (II) complexes. *J. Am. Chem. Soc.* **2006**, *128*, 12192–12204.

(25) Stoyanov, S. R.; Villegas, J. M.; Cruz, A. J.; Lockyear, L. L.; Reibenspies, J. H.; Rillema, D. P. Computational and spectroscopic studies of Re (I) bipyridyl complexes containing 2, 6-dimethylphenylisocyanide (CNx) ligand. *J. Chem. Theory Comput.* **2005**, *1*, 95–106.

(26) Fronzoni, G.; Stener, M.; Reduce, A.; Decleva, P. Time-dependent density functional theory calculations of ligand K edge and metal L edge X-ray absorption of a series of oxomolybdenum complexes. *J. Phys. Chem. A* **2004**, *108*, 8467–8477.

(27) Lapouge, C.; Cornard, J. Time dependent density functional theory study of electronic absorption properties of lead (II) complexes with a series of hydroxyflavones. *J. Phys. Chem. A* **2005**, *109*, 6752–6761.

(28) Ramaniah, L. M.; Boero, M. Structural, electronic, and optical properties of the diindenoperylene molecule from first-principles density-functional theory. *Phys. Rev. A* **2006**, *74*, 042505.

(29) Marinopoulos, A.; Wirtz, L.; Marini, A.; Olevano, V.; Rubio, A.; Reining, L. Optical absorption and electron energy loss spectra of carbon and boron nitride nanotubes: a first-principles approach. *Appl. Phys. A* **2004**, *78*, 1157–1167.

(30) Quartarolo, A. D.; Russo, N.; Sicilia, E. Structures and electronic absorption spectra of a recently synthesised class of photodynamic therapy agents. *Chem. Eur. J.* **2006**, *12*, 6797–6803.

(31) Varsano, D.; Di Felice, R.; Marques, M. A.; Rubio, A. A TDDFT study of the excited states of DNA bases and their assemblies. *J. Phys. Chem. B* **2006**, *110*, 7129–7138.

(32) Marques, M. A.; López, X.; Varsano, D.; Castro, A.; Rubio, A. Time-dependent density-functional approach for biological chromophores: the case of the green fluorescent protein. *Phys. Rev. Lett.* **2003**, *90*, 258101.

(33) Coe, B. J.; Harris, J. A.; Brunschwig, B. S.; Asselberghs, I.; Clays, K.; Garín, J.; Orduna, J. Three-dimensional nonlinear optical chromophores based on metal-to-ligand charge-transfer from ruthenium (II) or iron (II) centers. *J. Am. Chem. Soc.* **2005**, *127*, 13399–13410.

(34) Cave, R. J.; Burke, K.; Castner, E. W. Theoretical investigation of the ground and excited states of coumarin 151 and coumarin 120. *J. Phys. Chem. A* **2002**, *106*, 9294–9305.

(35) Jacquemin, D.; Perpète, E. A.; Scalmani, G.; Frisch, M. J.; Assfeld, X.; Ciofini, I.; Adamo, C. Time-dependent density functional theory investigation of the absorption, fluorescence, and phosphorescence spectra of solvated coumarins. *J. Chem. Phys.* **2006**, *125*, 164324.

(36) Jamorski, C. J.; Casida, M. E. Time-Dependent Density-Functional Theory Investigation of the Fluorescence Behavior as a Function of Alkyl Chain Size for the 4-(N, N-Dimethylamino) benzonitrile-like Donor- Acceptor Systems 4-(N, N-Diethylamino) benzonitrile and 4-(N, N-Diisopropylamino) benzonitrile. *J. Phys. Chem. B* **2004**, *108*, 7132–7141.

(37) Rappoport, D.; Furche, F. Photoinduced intramolecular charge transfer in 4-(Dimethyl) aminobenzonitrile- A Theoretical Perspective. *J. Am. Chem. Soc.* **2004**, *126*, 1277–1284.

(38) Tozer, D. J. Relationship between long-range charge-transfer excitation energy error and integer discontinuity in Kohn–Sham theory. *J. Chem. Phys.* **2003**, *119*, 12697–12699.

(39) Jamorski Jödicke, C.; Lüthi, H. P. Time-Dependent Density Functional Theory (TDDFT) Study of the Excited Charge-Transfer State Formation of a Series of Aromatic Donor- Acceptor Systems. *J. Am. Chem. Soc.* **2003**, *125*, 252–264.

(40) Stanton, J. F.; Gauss, J.; Ishikawa, N.; Head-Gordon, M. A comparison of single reference methods for characterizing stationary points of excited state potential energy surfaces. *J. Chem. Phys.* **1995**, *103*, 4160–4174.

(41) Cai, Z.-L.; Sendt, K.; Reimers, J. R. Failure of density-functional theory and time-dependent density-functional theory for large extended π systems. *J. Chem. Phys.* **2002**, *117*, 5543–5549.

(42) Grimme, S.; Parac, M. Substantial errors from time-dependent density functional theory for the calculation of excited states of large π systems. *ChemPhysChem* **2003**, *4*, 292–295.

(43) Tozer, D. J.; Amos, R. D.; Handy, N. C.; Roos, B. O.; Serrano-Andres, L. Does density functional theory contribute to the understanding of excited states of unsaturated organic compounds? *Mol. Phys.* **1999**, *97*, 859–868.

(44) Sobolewski, A. L.; Domcke, W. Ab initio study of the excited-state coupled electron–proton-transfer process in the 2-aminopyridine dimer. *Chem. Phys.* **2003**, *294*, 73–83.

(45) Dreuw, A.; Fleming, G. R.; Head-Gordon, M. Charge-transfer state as a possible signature of a zeaxanthin- chlorophyll dimer in the non-photochemical quenching process in green plants. *J. Phys. Chem. B* **2003**, *107*, 6500–6503.

(46) Slater, J. C. The theory of complex spectra. *Phys. Rev.* **1929**, *34*, 1293.

(47) Holøien, E. Radial configurational interaction in helium and similar atomic systems. *Phys. Rev.* **1956**, *104*, 1301.

(48) Koch, H.; Christiansen, O.; Jørgensen, P.; Olsen, J. Excitation energies of BH, CH2 and Ne in full configuration interaction and the hierarchy CCS, CC2, CCSD and CC3 of coupled cluster models. *Chem. Phys. Lett.* **1995**, *244*, 75–82.

(49) Gilbert, A. T.; Besley, N. A.; Gill, P. M. Self-consistent field calculations of excited states using the maximum overlap method (MOM). *J. Phys. Chem. A* **2008**, *112*, 13164–13171.

(50) Barca, G. M.; Gilbert, A. T.; Gill, P. M. Simple models for difficult electronic excitations. *J. Chem. Theory Comput.* **2018**, *14*, 1501–1509.

(51) Zhan, C.-G. Maximum overlap method and the bond strength. *Int. J. Quantum Chem.* **1987**, *32*, 1–11.

(52) Maksić, Z.; Eckert-Maksić, M.; Randić, M. Correlation between CH and CC spin-spin coupling constants and s character of hybrids calculated by the maximum overlap method. *Theor. Chim. Acta* **1971**, *22*, 70–79.

(53) Bartlett, R. J.; Öhrn, Y. How quantitative is the concept of maximum overlap? *Theor. Chim. Acta* **1971**, *21*, 215–234.

(54) Kobe, D. H. Maximum-Overlap Orbitals, an Energy Variational Principle, and Perturbation Theory. *Phys. Rev. C* **1971**, *3*, 417.

(55) Weinhold, F.; Brunck, T. The principle of maximum overlap. *J. Am. Chem. Soc.* **1976**, *98*, 3745–3749.

(56) Meldner, H.; Perez, J. Maximum-Ovelap Orbitals. *Phys. Rev. C* **1973**, *7*, 2158.

(57) Cioslowski, J.; Challacombe, M. Maximum similarity orbitals for analysis of the electronic excited states. *Int. J. Quantum Chem.* **1991**, *40*, 81–93.

(58) Hait, D.; Head-Gordon, M. Excited state orbital optimization via minimizing the square of the gradient: General approach and application to singly and doubly excited states via density functional theory. *J. Chem. Theory Comput.* **2020**, *16*, 1699–1710.

(59) Carter-Fenk, K.; Herbert, J. M. State-Targeted Energy Projection: A Simple and Robust Approach to Orbital Relaxation of Non-Aufbau Self-Consistent Field Solutions. *J. Chem. Theory Comput.* **2020**, *16*, 5067–5082.

(60) Yamaguchi, K.; Jensen, F.; Dorigo, A.; Houk, K. A spin correction procedure for unrestricted Hartree-Fock and Møller-Plesset wavefunctions for singlet diradicals and polyradicals. *Chem. Phys. Lett.* **1988**, *149*, 537–542.

(61) Saito, T.; Nishihara, S.; Kataoka, Y.; Nakanishi, Y.; Matsui, T.; Kitagawa, Y.; Kawakami, T.; Okumura, M.; Yamaguchi, K. Transition state optimization based on approximate spin-projection (AP) method. *Chem. Phys. Lett.* **2009**, *483*, 168–171.

(62) Saito, T.; Ito, A.; Watanabe, T.; Kawakami, T.; Okumura, M.; Yamaguchi, K. Performance of the coupled cluster and DFT methods for through-space magnetic interactions of nitroxide dimer. *Chem. Phys. Lett.* **2012**, *542*, 19–25.

(63) Ferré, N.; Guihéry, N.; Malrieu, J.-P. Spin decontamination of broken-symmetry density functional theory calculations: deeper insight and new formulations. *Phys. Chem. Chem. Phys.* **2015**, *17*, 14375–14382.

(64) Thompson, L. M.; Hratchian, H. P. Modeling the Photoelectron Spectra of MoNbO2–Accounting for Spin Contamination in Density Functional Theory. *J. Phys. Chem. A* **2015**, *119*, 8744–8751.

(65) Sheng, X.; Thompson, L. M.; Hratchian, H. P. Assessing the Calculation of Exchange Coupling Constants and Spin Crossover Gaps Using the Approximate Projection Model to Improve Density Functional Calculations. *J. Chem. Theory Comput.* **2019**, *16*, 154–163.

(66) Davidson, E. R. Spin-restricted open-shell self-consistent-field theory. *Chem. Phys. Lett.* **1973**, *21*, 565–567.

(67) Davidson, E. R.; Stenkamp, L. Z. SCF methods for excited states. *Int. J. Quantum Chem.* **1976**, *10*, 21–31.

(68) Saunders, V.; Hillier, I. A Level–Shifting method for converging closed shell Hartree–Fock wave functions. *Int. J. Quantum Chem.* **1973**, *7*, 699–705.

(69) Guest, M.; Saunders, V. R. On methods for converging open-shell Hartree-Fock wave-functions. *Mol. Phys.* **1974**, *28*, 819–828.

(70) McWeeny, R. SCF theory for excited states: I. Optimal orbitals for the states of a configuration. *Mol. Phys.* **1974**, *28*, 1273–1282.

(71) Brillouin, L. Actualités sci. et ind. *Nos* **1934**, *71*, 1933–1934.

(72) Bunge, C. F.; Jauregui, R.; Ley-Koo, E. Relativistic self-consistent-field atomic calculations using a generalization of Brillouin's theorem. *Can. J. Phys.* **1998**, *76*, 421–444.

(73) Coulson, C. Brillouin's theorem and the Hellmann-Feynman theorem for Hartree-Fock wave functions. *Mol. Phys.* **1971**, *20*, 687–694.

(74) Fischer, C. F. Hartree–Fock method for atoms. A numerical approach. **1977**,

(75) Hratchian, H. P. Communication: An efficient analytic gradient theory for approximate spin projection methods. 2013.

(76) Thompson, L. M.; Hratchian, H. P. Second derivatives for approximate spin projection methods. *J. Chem. Phys.* **2015**, *142*, 054106.

(77) Thompson, L. M.; Hratchian, H. P. Spin projection with double hybrid density functional theory. *J. Chem. Phys.* **2014**, *141*, 034108.

(78) Thompson, L. M.; Hratchian, H. P. On approximate projection models. *Mol. Phys.* **2019**, *117*, 1421–1429.

(79) Becke, A. *The quantum theory of atoms in molecules: from solid state to DNA and drug design*; John Wiley & Sons, 2007.

(80) Slater, J. C. A simplification of the Hartree-Fock method. *Phys. Rev.* **1951**, *81*, 385.

(81) Frisch, M. J.; Pople, J. A.; Binkley, J. S. Self-consistent molecular orbital methods 25. Supplementary functions for Gaussian basis sets. *J. Chem. Phys.* **1984**, *80*, 3265–3269.

(82) Raghavachari, K.; Trucks, G. W. Highly correlated systems. Excitation energies of first row transition metals Sc–Cu. *J. Chem. Phys.* **1989**, *91*, 1062–1065.

(83) McLean, A.; Chandler, G. Contracted Gaussian basis sets for molecular calculations. I. Second row atoms, Z= 11–18. *J. Chem. Phys.* **1980**, *72*, 5639–5648.

(84) Binning Jr, R.; Curtiss, L. Compact contracted basis sets for third-row atoms: Ga–Kr. *J. Comput. Chem.* **1990**, *11*, 1206–1216.

(85) Clark, T.; Chandrasekhar, J.; Spitznagel, G. W.; Schleyer, P. V. R. Efficient diffuse function-augmented basis sets for anion calculations. III. The 3-21+ G basis set for first-row elements, Li–F. *J. Comput. Chem.* **1983**, *4*, 294–301.

(86) Balabanov, N. B.; Peterson, K. A. Systematically convergent basis sets for transition metals. I. All-electron correlation consistent basis sets for the 3d elements Sc-Zn. *J. Chem. Phys.* **2005**, *123*.

(87) Kendall, R. A.; Dunning, T. H.; Harrison, R. J. Electron affinities of the first-row atoms revisited. Systematic basis sets and wave functions. *J. Chem. Phys.* **1992**, *96*.

(88) Prascher, B. P.; Woon, D. E.; Peterson, K. A.; Dunning, T. H.; Wilson, A. K. Gaussian basis sets for use in correlated molecular calculations. VII. Valence, core-valence, and scalar relativistic basis sets for Li, Be, Na, and Mg. *Theor. Chem. Acc.* **2011**, *128*.

(89) Wilson, A. K.; Woon, D. E.; Peterson, K. A.; Dunning, T. H. Gaussian basis sets for use in correlated molecular calculations. IX. The atoms gallium through krypton. *J. Chem. Phys.* **1999**, *110*.

(90) Woon, D. E.; Dunning, T. H. Gaussian basis sets for use in correlated molecular calculations. III. The atoms aluminum through argon. *J. Chem. Phys.* **1993**, *98*.

(91) Pritchard, B. P.; Altarawy, D.; Didier, B.; Gibsom, T. D.; Windus, T. L. A New Basis Set Exchange: An Open, Up-to-date Resource for the Molecular Sciences Community. *J. Chem. Inf. Model.* **2019**, *59*.

(92) Feller, D. The role of databases in support of computational chemistry calculations. *J. Comput. Chem.* **1996**, *17*.

(93) Schuchardt, K. L.; Didier, B. T.; Elsethagen, T.; Sun, L.; Gurumoorthi, V.; Chase, J.; Li, J.; Windus, T. L. Basis Set Exchange: A Community Database for Computational Sciences. *J. Chem. Inf. Model.* **2007**, *47*.

(94) Frisch, M. J.; Trucks, G. W.; Schlegel, H. B.; Scuseria, G. E.; Robb, M. A.; Cheeseman, J. R.; Scalmani, G.; Barone, V.; Petersson, G. A.; Nakatsuji, H.; Li, X.; Caricato, M.; Marenich, A.; Bloino, J.; Janesko, B. G.; Gomperts, R.; Mennucci, B.; Hratchian, H. P.; Ortiz, J. V.; Izmaylov, A. F.; Sonnenberg, J. L.; Williams-Young, D.; Ding, F.; Lipparini, F.; Egidi, F.; Goings, J.; Peng, B.; Petrone, A.; Henderson, T.; Ranasinghe, D.; Zakrzewski, V. G.; Gao, J.; Rega, N.; Zheng, G.; Liang, W.; Hada, M.; Ehara, M.; Toyota, K.; Fukuda, R.; Hasegawa, J.; Ishida, M.; Nakajima, T.; Honda, Y.; Kitao, O.; Nakai, H.; Vreven, T.; Throssell, K.; Montgomery, J. A.; Jr.,; Peralta, J. E.; Ogliaro, F.; Bearpark, M.; Heyd, J. J.; Brothers, E.; Kudin, K. N.; Staroverov, V. N.; Keith, T.; Kobayashi, R.; Normand, J.; Raghavachari, K.; Rendell, A.; Burant, J. C.; Iyengar, S. S.; Tomasi, J.; Cossi, M.; Millam, J. M.; Klene, M.; Adamo, C.; Cammi, R.; Ochterski, J. W.; Martin, R. L.; Morokuma, K.; Farkas, O.; Foresman, J. B.; ; Fox, D. J. Gaussian Development Version Revision I.09. 2016; Gaussian Inc. Wallingford CT.

(95) Hratchian, H.; Schlegel, H. Theory and Applications of Computational Chemistry: The First 40 Years. *Dykstra, CE* **2005**, 195–249.

(96) Huber, K.-P.; Herzberg, G. *Molecular spectra and molecular structure: IV. Constants of diatomic molecules*; Springer Science & Business Media, 1979.

(97) Herzberg, G. Molecular spectra and molecular structure. Vol. III: Electronic spectra and electronic structure of polyatomic molecules. *New York: Van Nostrand, Reinhold, 1966* **1966**,

(98) Bencheikh, M.; Koivisto, R.; Launila, O.; Flament, J. The low-lying electronic states of CrF and CrCl: Analysis of the A 6 Σ+ X 6 Σ+ system of CrCl. *J. Chem. Phys.* **1997**, *106*, 6231–6239.

(99) Clouthier, D.; Ramsay, D. The spectroscopy of formaldehyde and thioformaldehyde. *Ann. Rev. Phys. Chem.* **1983**, *34*, 31–58.

(100) Dong, R.; Nanes, R.; Ramsay, D. Rotational analyses of bands of the system of cis-glyoxal. *Can. J. Chem.* **1993**, *71*, 1595–1597.

(101) Brand, J. C. D.; Williamson, D. Near-ultra-violet spectrum of propenal. *Discuss. Faraday Soc.* **1963**, *35*, 184–191.

(102) Birge, R. R.; Pringle, W. C.; Leermakers, P. A. Excited-state geometries of the singly substituted methylpropenals. I. Vibrational-electronic analysis of S1 (n,. pi.*). *J. Am. Chem. Soc.* **1971**, *93*, 6715–6726.

(103) Hadad, C. M.; Foresman, J. B.; Wiberg, K. B. Excited states of carbonyl compounds. 1. Formaldehyde and acetaldehyde. *J. Phys. Chem.* **1993**, *97*, 4293–4312.

(104) Clouthier, D. J.; Karolczak, J. A pyrolysis jet spectroscopic study of the rotationally resolved electronic spectrum of dichlorocarbene. *J. Chem. Phys.* **1991**, *94*, 1–10.

(105) Cai, Z.-L.; Bai, J.-L. Theoretical studies of the electronic spectrum of SiF2. *Chem. Phys.* **1993**, *178*, 215–221.

(106) Bagus, P. S. Self-Consistent-Field Wave Functions for Hole States of Some Ne-Like and Ar-Like Ions. *Phys. Rev.* **1965**, *139*, A619–A634.

(107) Bagus, P. S.; Illas, F. Orbitals Permit the Interpretation of Core-Level Spectroscopies in Terms of Chemistry. *Catal. Lett.* **2020**, 1–7.

(108) Barca, G. M.; Gilbert, A. T.; Gill, P. M. Excitation number: Characterizing multiply excited states. *J. Chem. Theory Comput.* **2018**, *14*, 9–13.

(109) Besley, N. A.; Gilbert, A. T.; Gill, P. M. Self-consistent-field calculations of core excited states. *J. Chem. Phys.* **2009**, *130*, 124308.

(110) Deng, J.; Gilbert, A. T.; Gill, P. M. Rydberg states of the helium atom. *Int. J. Quantum Chem.* **2009**, *109*, 1915–1919.

(111) Barca, G. M.; Gilbert, A. T.; Gill, P. M. Communication: Hartree-Fock description of excited states of H2. 2014.

(112) Loos, P.-F.; Scemama, A.; Blondel, A.; Garniron, Y.; Caffarel, M.; Jacquemin, D. A mountaineering strategy to excited states: Highly accurate reference energies and benchmarks. *J. Chem. Theory Comput.* **2018**, *14*, 4360–4379.

(113) Corzo, H.; Velasco, A.; Lavín, C.; Ortiz, J. MgH Rydberg series: Transition energies from electron propagator theory and oscillator strengths from the molecular quantum defect orbital method. *J. Quant. Spectrosc. Radiat. Transfer* **2018**, *206*, 323–327.

(114) Daul, C. Density functional theory applied to the excited states of coordination compounds. *Int. J. Quantum Chem.* **1994**, *52*, 867–877.

(115) Ziegler, T.; Rauk, A.; Baerends, E. J. On the calculation of multiplet energies by the Hartree-Fock-Slater method. *Theor. Chim. Acta* **1977**, *43*, 261–271.

(116) Noodleman, L.; Davidson, E. R. Ligand spin polarization and antiferromagnetic coupling in transition metal dimers. *Chem. Phys.* **1986**, *109*, 131–143.